

Direct Blow-Spinning of Nanofibers on a Window Screen for Highly Efficient PM_{2.5} Removal

Bilal Khalid,^{†,§} Xiaopeng Bai,^{†,§} Hehe Wei,[†] Ya Huang,[†] Hui Wu,^{*,†} and Yi Cui^{*,‡}

[†]State Key Laboratory of New Ceramics and Fine Processing, School of Materials Science and Engineering, Tsinghua University, Beijing 100084, China

[‡]Department of Materials Science and Engineering, Stanford University, Stanford, California 94305, United States

Supporting Information

ABSTRACT: Particulate matter (PM) pollution has caused many serious public health issues. Whereas indoor air protection usually relies on expensive and energy-consuming filtering devices, direct PM filtration by window screens has attracted increasing attention. Recently, electrospun polymer nanofiber networks have been developed as transparent filters for highly efficient PM_{2.5} removal; however, it remains challenging to uniformly coat the nanofibers on window screens on a large scale and with low cost. Here, we report a blow-spinning technique that is fast, efficient, and free of high voltages for the large-scale direct coating of nanofibers onto window screens for indoor PM pollution protection. We have achieved a transparent air filter of 80% optical transparency with >99% standard removal efficiency level for PM_{2.5}. A test on a real window (1 m × 2 m) in Beijing has proven that the nanofiber transparent air filter acquires excellent PM_{2.5} removal efficiency of 90.6% over 12 h under extremely hazy air conditions (PM_{2.5} mass concentration > 708 μg/m³). Moreover, we show that the nanofibers can be readily coated on the window screen for pollution protection and can be easily removed by wiping the screen after hazardous days.

KEYWORDS: PM_{2.5}, nanofibers, window filtration, transparent, indoor protection, blow spinning



Particle pollution, also called particulate matter (PM), is a mixture of solids and liquid droplets floating in the air. Some particles are released directly from a specific source, whereas others form in complicated chemical reactions in the atmosphere. Nowadays, PM has become a matter of serious concern due to its enormous threat to public health, especially in developing countries like India and China. Moreover, its extremely high concentration in air badly affects visibility, climate forcing, direct sunlight, and ecosystems.^{1–7} PM composition suggests that it carries very tiny particles and droplets of liquid.⁸ However, it is mainly classified into two types on the basis of size as PM_{2.5} and PM₁₀, referring to particle sizes below 2.5 μm and between 2.5 and 10 μm, respectively. PM_{2.5} is particularly hazardous due to its extremely small size, which can easily penetrate into human lungs and bronchi.⁹ Frequent exposure to such hazy weather conditions can cause deleterious health issues like stroke, cancer, heart failure, and lung infections,^{10–14} and short-term exposure to a highly polluted PM environment can create a serious risk of asthmatic problems. At present, a large number of coal-based industries in many developing countries like China are responsible for creating such high PM pollution. On extremely hazy days, visibility is decreased significantly and becomes even worse at night. During such hazy weather, the air quality reaches its worst level because of a high concentration of PM

pollution. Individually, people tackle this problem by using mask filters of various qualities as protective tools during outdoor activities. However, such masks are bulky and resistant to air flow.¹⁵ In the case of indoor commercial buildings, protection is usually provided by a sophisticated ventilation system or by a central air conditioning network. In contrast, common residential buildings are seldom equipped with such PM filtering systems. Furthermore, an enormous amount of energy is always required for substantial pumping to exchange active air through mechanical ventilation.¹⁶

Quality and exchange of indoor air is also a matter of great concern while people are staying indoors.¹⁷ It would be perfect if passive air exchange could be accomplished through natural ventilation of window mesh for indoor air filtration. Windows with high surface area always facilitate efficient air exchange for indoor purposes. The idea of coating a window mesh with a suitable fibrous layer owing to not only capture high amounts of PM but that is also highly transparent to the sunlight and sight viewing at the same moment would be of greater interest. Herein, we introduce a new blow spin methodology to create transparent air filters for indoor protection of windows for the

Received: November 14, 2016

Revised: December 19, 2016

Published: December 27, 2016

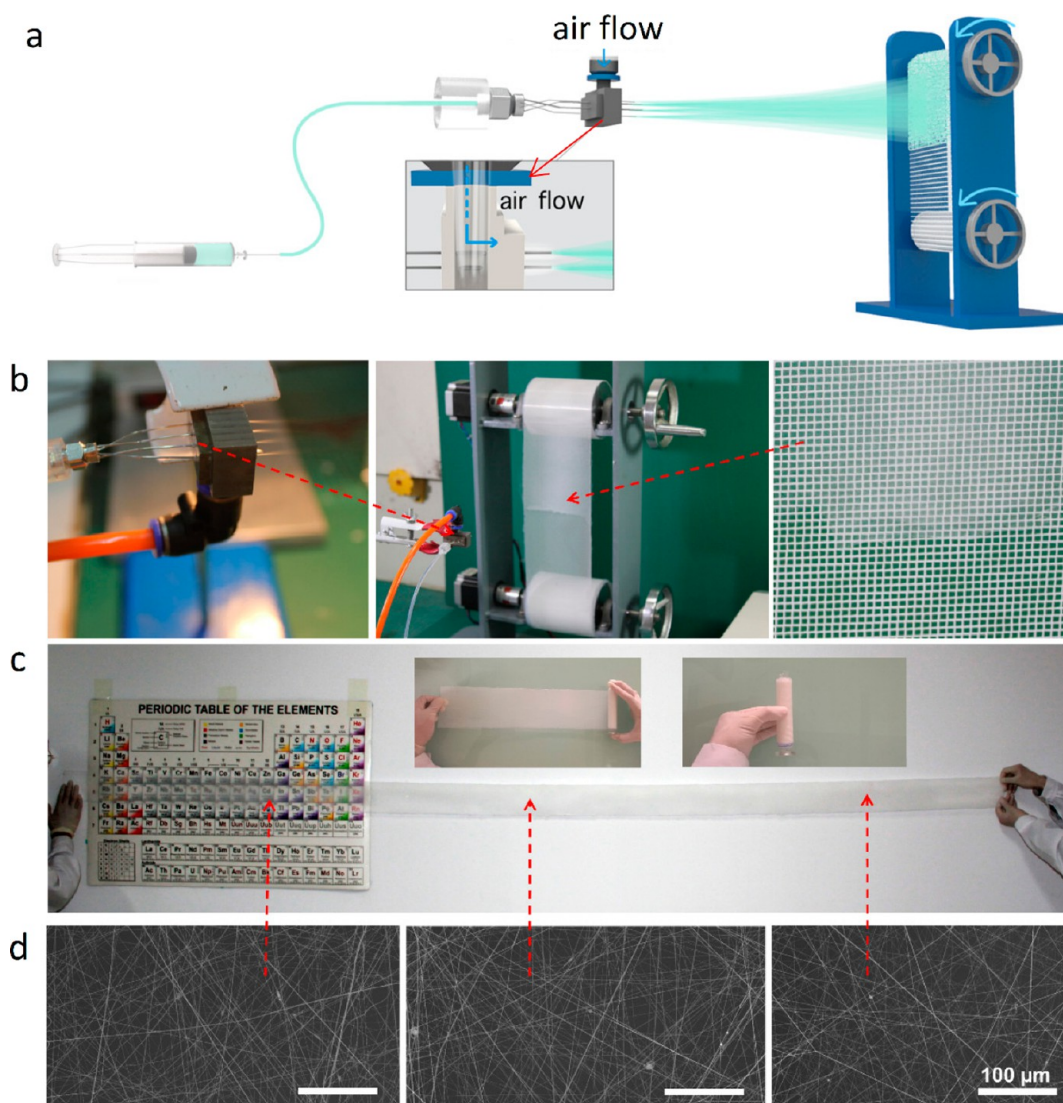


Figure 1. Roll-to-roll production of nanofibers. (a) Experimental arrangement for roll-to-roll deposition of nanofibers. (b) Sequential multineedle blow spinning on rolling polymeric mesh of larger size and successful deposition of fibers. (c) Transparency check of the deposited fibers and their binding adhesion and efficacy test in terms of folding and subsequent opening. (d) SEM images of the blow-spun fibers taken from three different places of the coated rolling mesh, showing superb distribution and uniformity. Scale bar is 100 μm .

first time in science history. $\text{PM}_{2.5}$ has a complicated composition, carrying organic matter in the form of elemental carbon and organic carbon, whereas the inorganic portion is mainly comprised of SiO_2 , SO_4^{2-} , and NO_3^- . The origins of these diverse compositions of $\text{PM}_{2.5}$ are thought to be vehicular emissions, industrial emissions, secondary aerosols, coal combustion, soil dust, and biomass burning.^{18–21} This behavior of PM suggests that it could effectively be removed by fiber membranes with suitable surface functionalities and altered chemistry. Therefore, essential components of PM can be readily removed by filtration membrane technology. Recently, researchers found that polar polymeric nanofiber membranes like polyacrylonitrile (PAN), nylon, and polyimide have much higher PM removal efficiency as compared to that of nonpolar polypropylene fibers that are used in existing filtration membranes.^{22–24} The high capture ability of the polar polymeric nanofiber membrane makes it possible to use a thin nanofiber membrane on a real window mesh, which can be highly transparent and low air flow resistant. Earlier technologies for the production of nanofibers include solution

spinning and melt blowing;^{25,26} however, each of these has its own disadvantages. Electrospinning is thought to have the most potential and be a reliable method of commercial nanofibers fabrication.²⁷ However, low mass production, risk of high voltages, solvent compatibility regarding dielectric constant, complicated operating conditions, and long run time are its serious hurdles for coating the high surface area real window mesh.

With all of these factors in consideration, we developed a new blow spin methodology for the production of a real window transparent air filter. This methodology is not only free from the use of high voltages but also quick, highly yielding, and easy to operate. Moreover, by adjusting all these parameters, we have successfully coated a real window mesh of 29×133 cm dimensions with a fine layer of PAN nanofibers. In our real window transparent air filter test, we have successfully achieved smooth removal efficiencies of 92.6, 91.2, and 90.6% for PM_{10} , $\text{PM}_{10-2.5}$, and $\text{PM}_{2.5}$ over a time duration of 12 h under an extremely hazy air quality of $\text{PM}_{2.5}$ index $> 708 \mu\text{g}/\text{m}^3$.

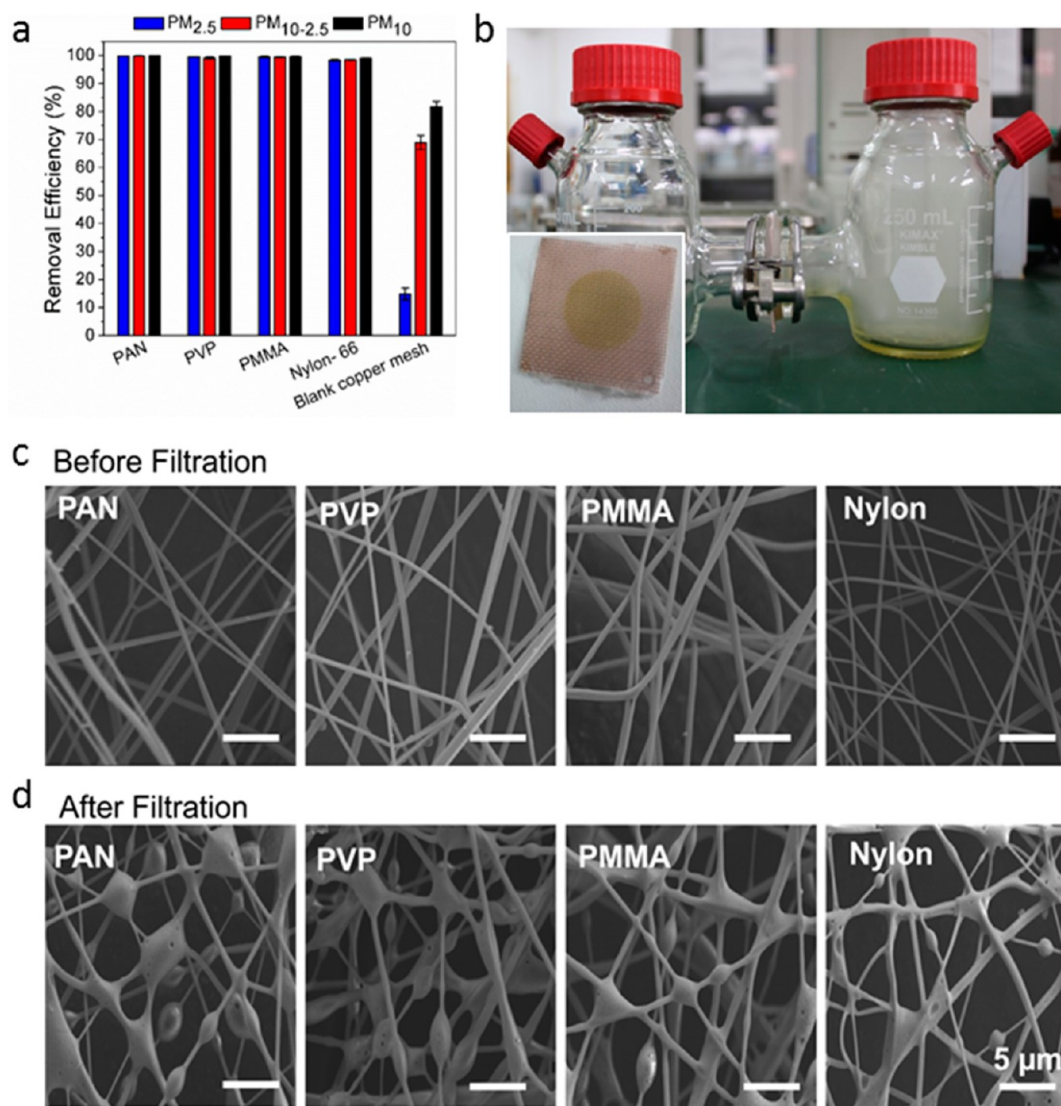


Figure 2. Various polymeric filters with their PM_{2.5} capturing abilities. (a) Comparison of highest filtering performance of PAN, PVP, PMMA, and Nylon-66 including blank copper mesh under similar conditions for the PM levels. Error bar denotes the standard deviation of three replicate values. (b) Pictorial representation of successful blocking of the PM from outdoors (right bottle) to indoors (left bottle). (c) SEM images of PAN, PVP, PMMA, and Nylon-66 before filtration. (d) SEM images of PAN, PVP, PMMA, and Nylon-66 transparent air filters elucidating PM capture after filtration. Scale bar is 5 μm .

One of the prime objective of our recent work was the large-scale production of the air filters in a quick and easy way. For this reason, we turned our recent research focus toward developing a novel roll-to-roll single step method without any pre- or post-treatment. Furthermore, the key advantages of our designed roll-to-roll method are free of using high voltages and metallic targets as compared to electrospinning. Figure 1a depicts the graphical arrangement of the whole roll-to-roll experimental setup. Figure 1b elaborates the sequential multineedle blow spinning on to a rolling polymeric mesh kept a certain distance from the needle. For this particular rolling experiment, a commercial Nylon mesh is used due its flexible nature to facilitate continuous rolling and its subsequent opening. Secondly, its stability against DMF at room temperature is another key factor for its selection. PAN with DMF has been used as a fiber coating material. Continuous blowing of the PAN solution onto this polymeric mesh, rolling at a certain speed, has resulted in a successful uniformly arranged transparent fiber coating. Through this rolling process,

a large scale deposition of fibers on 2.5 m long polymeric mesh has been successfully achieved in a short time of 3 min. It was observed that rolling of the mesh into many folds did not affect the structure and physical appearance of the fibers at all. For this specific cause, a rolling test of the as obtained coated polymeric mesh was conducted in the lab. Figures 1c shows that the coated polymeric mesh was rolled into many folds and opened again, which clearly shows no damage to the fibers. Moreover, the first part of Figure 1c clearly indicates the high optical transparency of the deposited fibers. For more structural morphological examination, three different parts of the polymeric mesh were selected after the rolling test and subjected to SEM examination on a larger scale bar. It is clear from Figure 1d that during the roll-to-roll production, and even after the rolling test, there was no prominent damage happened to the internal or outer morphologies of the fibers. Moreover, deposited fibers were uniformly distributed over all the mesh area. This ensures that our new strategy of large-scale

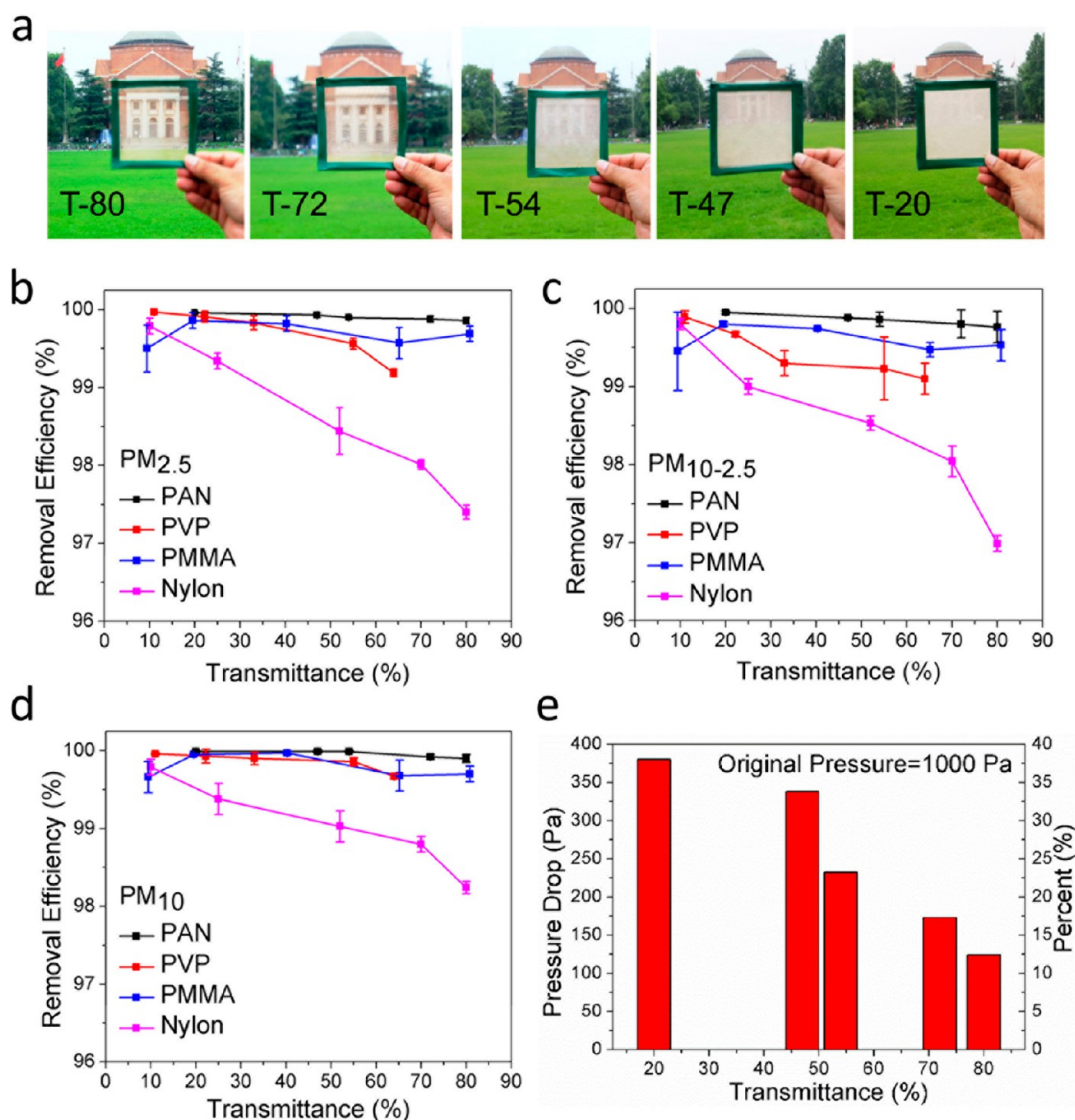


Figure 3. Transparency and pressure drop evaluation of the air filters. (a) Photographs showing the diverse transparency levels of PAN transparent air filters. (b) Comparison of PM_{2.5} removal efficiencies of PAN, PVP, PMMA, and Nylon-66 at various transmittances. (c) Comparison of PM_{10-2.5} removal efficiencies of PAN, PVP, PMMA, and Nylon-66 at various transmittances. (d) Comparison of PM₁₀ removal efficiencies of PAN, PVP, PMMA, and Nylon-66 at various transmittances. Error bar shows the standard deviation of three repeated values. (e) Illustration of pressure drop with respect to various transmittances of PAN transparent air filters.

roll-to-roll production of transparent air filters is not only quick but also effective in terms of a morphological point of view.

Selection of various polymers for lab scale experiments was made on the bases of dipole moments,²² and their PM capturing abilities were investigated. The blow spin methodology was applied to fabricate the polymeric fibrous air filters. It has unique advantages such as being free from high voltages and the risk of metallic targets to form a uniform membrane with a controllable diameter. This feature of blow spinning makes it an ideal tool for the production of transparent air filters. Steady air flow must be maintained behind the tip of the syringe containing the polymer solution. The applied air flow drags the polymer solution into fine nanofibers and deposits them on a target, which is a commercial copper mesh in this experiment. As a result of blowing air, blow spun nanofibers of polymeric solutions were deposited across the holes of the mesh to form a continuous fibrous network. This blow spinning method is superbly scalable and can easily be applied to real window mesh. The resulting transparent nanofibrous air filter is

mechanically robust. Air filters with different polymers of varying transparency were prepared by time scaled experiments. Commonly available polymers like polyacrylonitrile (PAN), polyvinylpyrrolidone (PVP), poly(methyl methacrylate) (PMMA), and Nylon-66 with low cost were chosen.

In the present research, smoke was generated by burning fragrance incense sticks. Appropriate burning of incense can produce PM of more than 45 mg g⁻¹. The exhaust smoke is comprised of many gaseous pollutants, including NO₂, CO, SO₂, CO₂, and some volatile organic compounds such as benzene, xylene, toluene, ketones, aldehydes, and polycyclic aromatic hydrocarbons. The composition of this smoke is nearly the same as that of extremely polluted air during a hazy day. Quantitative removal analysis of PM_{2.5}, PM_{10-2.5}, and PM₁₀ of various filters is shown in Figure 2a. From the removal efficiency comparison, it is evident that PAN has the highest removal efficiencies for all PM_{2.5}, PM_{10-2.5}, and PM₁₀ than those of PVP, PMMA, Nylon-66, and ordinary copper mesh. The removal efficiencies were calculated by comparing the

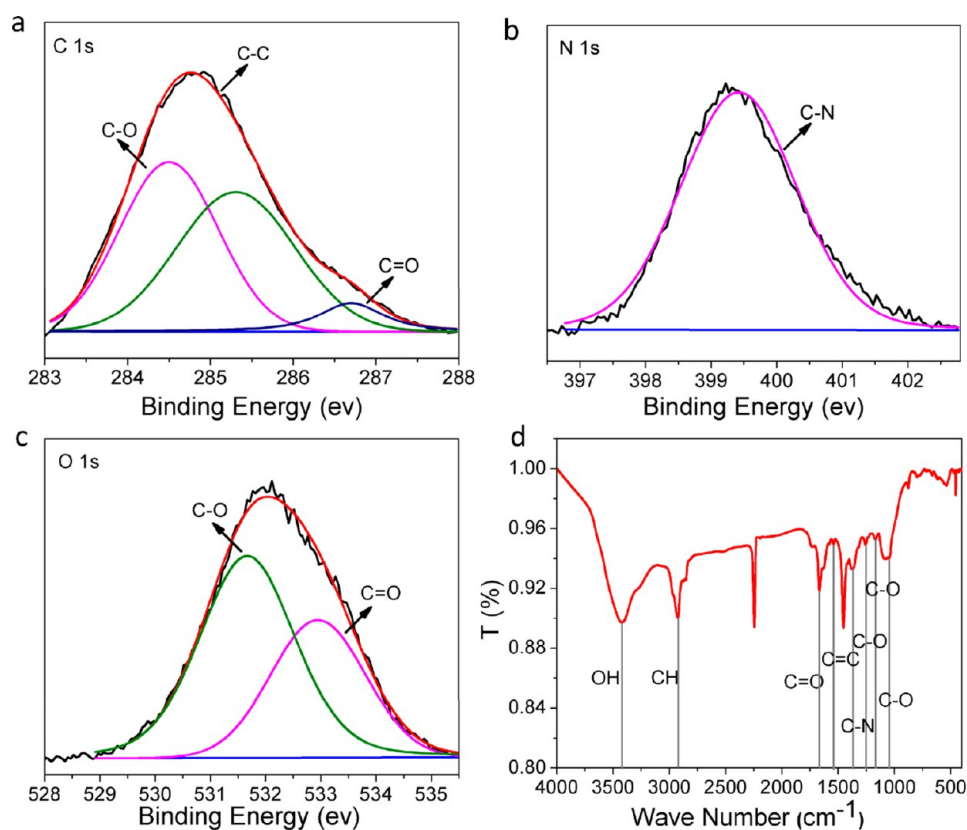


Figure 4. Compositional analysis of PM-based smoke. (a–c) XPS elemental characterization of captured PM smoke particles illustrating C 1s, O 1s, and N 1s peak analysis. (d) FTIR demonstration of PM particles indicating the presence of various functional groups.

particle concentration before and after filtration. The obtained results suggest that the polymer with the higher dipole moment has a greater ability to bind the PM and hence increases the removal efficiency. This phenomenon suggests that dipole–dipole or induced dipole interactions can greatly enhance the binding of PM with the fiber’s surface. However, lower transmittance with higher packing density is another prominent factor of increased efficiency. With a transmittance value of 20%, the PAN filter shows the highest removal efficiencies of 99.95 ± 0.02 , 99.96 ± 0.01 , and $99.99 \pm 0.01\%$ for $PM_{2.5}$, $PM_{10-2.5}$, and PM_{10} , respectively. These results demonstrated that PAN has better surface properties than those of PVP, PMMA, Nylon-66, and metallic mesh; furthermore, PAN removal efficiencies in all three cases of PM sizes are also higher than the standard removal level of >95%. Figure 2b provides a demonstration of stopping PM pollution. A hazardous level of $PM_{2.5}$ index > 500 or $PM_{2.5}$ mass concentration > $416.66 \mu\text{g}/\text{m}^3$ was generated by burning incense, and a PAN filter with 54% transmittance was placed in the connection of two bottles. As it is evident from Figure 2b, the left bottle is still clear, and a test of the $PM_{2.5}$ level after 10 min resulted in a good PM level of <5. This ensures the brilliant efficacy of the PAN transparent air filter.

Scanning electron microscopy (SEM) was applied to investigate the structural morphology and detailed interactions of PM with each filter, including PAN, PVP, PMMA, and Nylon-66 before and after capturing the PM. Panels c and d in Figure 2 depict the general capturing mechanism of PM soft particles by nanofibers. These images show that nanofibrous-based filters of each polymer have similar morphologies with fiber diameters of 150–250 nm with similar uniform packing

densities. Investigation of these images reveals that the number and density of as captured PM by PAN filters were both greater than those of other polymers. A deeper look suggests that the smoke containing PM strongly wrapped the surface of each fiber to form an initial layer coating, which subsequently turned into stable spherical shapes at the junctions of the fibers. It is obvious from the Figure S1 that the diameter of each polymer increased from 150 to 200 nm to several hundred nm after filtration.

Aside from the capturing ability of the air filter, its ability to transmit sunlight is another significant parameter that has also been evaluated. Figure 3a provides photographs of the PAN transparent air filters with transmittances of approximately 80, 72, 54, 47, and 20%. A deeper look at Figure 3a suggests that the transmitted light views of the historical Tsinghua building through the filters with transmittances of approximately 80 and 72% are very clear. However, from the transmittance level of ~54%, it begins to become blurry and reaches its maximum at ~20%. Obviously it is more difficult for transmitted light to penetrate through the filters with greater thickness and lower transmittance as compared to ordinary sunlight, so in this case it results in a blurry view. These finding prompted us to coat our real window mesh at an optimum transmittance level such that there will be reasonable views outside as well easy penetration of sunlight inside the room. The PM removal efficiencies of all four polymers were evaluated at their various transmittance values, and the results are depicted in Figure 3(b–d). An inspection of these graphs suggests that there is an increasing trend of $PM_{2.5}$ capturing efficiency with decreasing fiber transmittance level from 80 to 20% of PAN. For the PAN filter, an excellent removal efficiency level of >99% has been

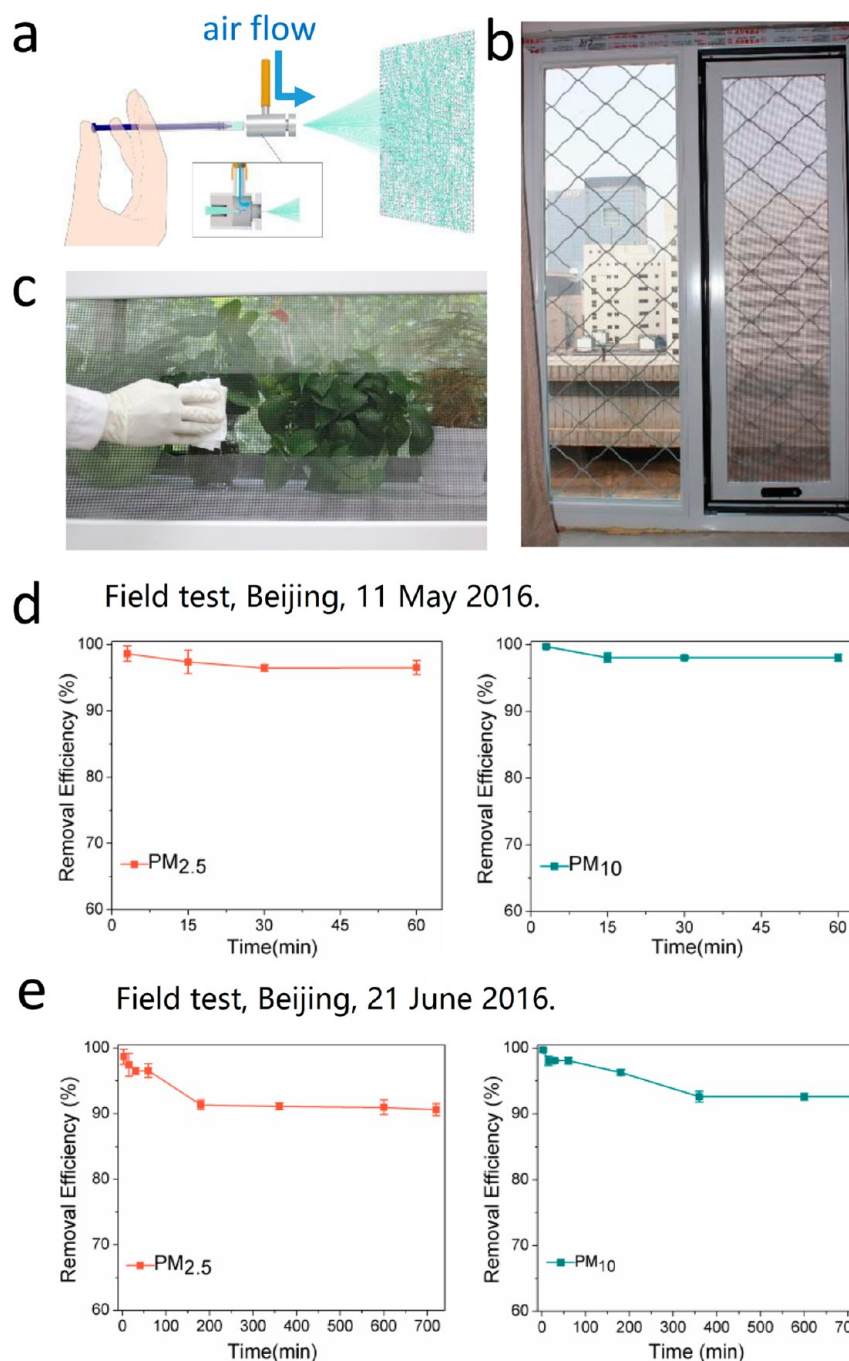


Figure 5. Real window-based PM filtering performances. (a) Practical model of the blow-spinning setup for the window screen coating. (b) Real window consisting of a removable metallic screen coated with PAN blow-spun fibers. (c) Successful wiping of nanofibers from the window screen with the help of tissue paper. (d) Field test conducted on May 11th, 2016 to calculate the filtering performance of the PAN-coated window screen for PM_{2.5} and PM₁₀ over a time duration of 1 h under extremely hazy weather conditions of the PM_{2.5} level of $\geq 708 \mu\text{g}/\text{m}^3$. (e) Repeated field test conducted on June 21st, 2016 to ensure the filtering performance of the PAN-coated window screen for PM_{2.5} and PM₁₀ for a longer time duration of 12 h on an extremely hazy day with PM_{2.5} level $\geq 708 \mu\text{g}/\text{m}^3$.

successfully obtained at all optical transmittance levels of 20–80%. A >95% standard removal efficiency level for PM_{2.5}, PM_{10–2.5}, and PM₁₀ was also achieved by both PVP and PMMA at lower transmittance of $\sim 64\%$. Nylon-66 also exhibits the removal efficiencies of 97.4, 97, and 98.24% for PM_{2.5}, PM_{10–2.5}, and PM₁₀, respectively, at lower transmittance of $\sim 80\%$. This also meets the standard removal efficiency level of >95%. Commercial copper mesh of $1 \times 1 \text{ mm}$ pore size has also been tested for PM_{2.5}, PM_{10–2.5}, and PM₁₀ under the same

conditions, and the results are depicted in Figure S2, which indicates that the removal efficiencies of original copper mesh are very small as compared to those coated with fibers of various polymers.

Other than high removal efficiency, retaining high air flow and its penetration is another important feature when evaluating the performance of an air filter. A quantitative test of the air flow was carried out by measuring the pressure drop (Δp) of every PAN air filter at each transmittance. The

pressure difference was calculated across the air filter under a steady flow of air of 0.6–0.8 m/s with an original air pressure of 1000 Pa. Table S1 shows that the pressure drops for PAN air filters with 80 and 72% transparency are only 124 and 173 Pa, respectively. This pressure drop is almost comparable to that of a blank window screen, which is around 139 Pa. Figure 3e shows a trend of increasing pressure drop (Δp) with decreasing transmittance or filter thickness and vice versa. The overall performance of the transparent PAN air filters including both efficiency and pressure drop was assessed by quality factor (Q.F). Table S1 shows that all five PAN transparent air filters have effective quality factors.

X-ray photoelectron spectroscopy (XPS) was carried out to investigate the composition and surface chemistry with deep elemental analysis of the smoke-captured PM. It is shown in Figure 4a that the C 1s signal for surface-detected elemental composition of smoke PM is comprised of three major peaks. Peaks at 284.5, 285.3, and 286.7 eV correspond to C–C, C–O, and C=O bonds, respectively. Figure 4b elaborates that the peaks of O 1s are also in accordance with peaks of C 1s, hence showing the existence of C–O and C=O bonds around 532.9 and 531.6 eV, respectively. Other than C and O, a small fraction of N has also been detected in smoke PM. Only one peak represented in Figure 4c relates to N 1s and appears around 399.4 eV. The overall XPS analysis suggests that the surface of smoke PM mainly consists of three major elements, C, O, and N, and their ratio is 78.55, 14.47, and 6.98%, respectively. For the existence of various functional groups present in smoke PM to be investigated more thoroughly, FTIR analysis was carried out. Figure 4d shows that the broad band peak at 3417 cm^{-1} corresponds to O–H, whereas a sharp peak at 2923 cm^{-1} indicates the presence of C–H bonds. The other peaks of FTIR spectra at 1660, 1533, 1367, 1259, 1172, and 1056 present the existence of C=O, C=C, C–N, and C–O functional groups, respectively.

For ensuring the removal efficiency and efficacy of our transparent air filters in real practical life, a window-based experiment was conducted for the first time in one of the room of Tsinghua University in Beijing, China on May 11th, 2016. Literature shows that 40.7% of Beijing's PM contains organic matter,²⁸ which is in very good agreement with our experimental conditions performed in the bottle apparatus. The $\text{PM}_{2.5}$ mass concentration on that particular day was detected to be at an extremely hazardous level of $>708 \mu\text{g}/\text{m}^3$. Figure 5a shows an experimental blow-spinning setup, which was particular aimed to coat the window screen with PAN blow-spun fibers. Because of better surface chemistry, excellent adhesion ability, higher dipole moment, and better environmental stability among PVP, PMMA, and Nylon, PAN was chosen as the window screen filter. PVP, which is sensitive to moisture under extremely humid conditions, was avoided. However, lab-scale findings of PVP suggest that it can still be used as a window filter under extremely dry weather conditions such as in Beijing. A special iron-coated window mesh was selected for this particular experiment. This may not only lower the risk of direct adsorption and absorption of solvent during blow spinning but also minimize the absorption of the minute quantity of the solvent remaining in the fibers after sticking onto the mesh. Figure 5b displays the actual window with removable screen of $133 \times 29 \text{ cm}$, and Figure 5c depicts an easy wiping demonstration of the fibers from the window screen in daily life using tissue paper after hazardous days. At first, whole room air was cleaned up to $\text{PM}_{2.5}$ index of ~ 52 on that

particular hazy day with the help of an internal air filter. After a steady internal value of the $\text{PM}_{2.5}$ index was maintained, the window was opened and the door was kept closed. This test was conducted to test the blocking ability of the uncoated original window mesh. Figure S3 shows that the ordinary window mesh was only capable of stopping 42.3, 48.12, and 50% of $\text{PM}_{2.5}$, $\text{PM}_{10-2.5}$, and PM_{10} of outside polluted air. However, a considerable proportion of $\text{PM}_{2.5}$, $\text{PM}_{10-2.5}$, and PM_{10} in the form of 57.7, 51.88, and 50% could still easily penetrate through the bare window mesh in a quick time of 10 min. To test the real window-based filtering performance of our transparent air filter, the same mesh was coated through an arranged blow spinning setup (Figure 5a) with a fine layer of PAN nanofibers and subsequently inserted in the same window (Figure 5b). The environment of the room was again cleaned to $\text{PM}_{2.5}$ index ~ 52 in a similar fashion as described earlier. The window was reopened, and removal efficiencies were calculated for $\text{PM}_{2.5}$, PM_{10} , and $\text{PM}_{10-2.5}$ at different time intervals up to 1 h (60 min). Figure 5d and Figure S5 demonstrate that smooth filtering efficiencies of 96.5, 98.08, and 96.7% were successfully achieved for $\text{PM}_{2.5}$, PM_{10} , and $\text{PM}_{10-2.5}$, respectively, for time durations of 15 to 60 min at first. However, to confirm the tremendous filtering performance and eliminate doubts and omissions of our real window field test, this field test was again conducted in a similar fashion on June 21st, 2016 under an extremely hazy day with $\text{PM}_{2.5}$ mass concentration $>708 \mu\text{g}/\text{m}^3$. This time experiment was aimed to continue up to 12 h to check the repeatability as well ensure the efficacy of the filter for a longer period of time. Figure 5e and Figure S6 clearly demonstrate that the removal efficiencies for $\text{PM}_{2.5}$, PM_{10} , and $\text{PM}_{10-2.5}$ were not only still $>90\%$ after 12 h but were also consistent with the first 60 min results obtained from the previously conducted field test on May 11th, 2016. This phenomenon concludes the excellent repeatability, filtering performance, and efficacy of the continuous 12 h field test of the PAN-based real window transparent air filter. Undoubtedly, these findings have opened new cost-effective directions for a user friendly and easy way to provide a healthier indoor environment during extremely hazy days. Figure S4 also shows a comparison of removal efficiencies of a blank window screen and that coated with blow-spun nanofibers. This comparison confirms the excellent filtering efficiency and performance of our window screen transparent air filter in extremely hazy weather. Moreover, Figure S7 demonstrates the successful capturing of both organic and inorganic PM particles from natural outdoor air, hence preventing their ultimate penetration to the indoor room through the window screen.

We have demonstrated a new methodology called blow spinning for the fabrication of blow-spun polymer nanofibers. Such blowspun fibers with their small diameter and optimized surface chemistry are highly effective as transparent PM filters. These filters have proven to be very effective for blocking PM from entering the indoor environment, hence providing natural ventilation with optimum optical transparency. This has been proven practically by installing the blow-spun fibers on a real window screen to obtain a minimum 90.6% removal efficiency of $\text{PM}_{2.5}$ in extremely hazardous weather over 12 h. Moreover, the addition of roll-to-roll blow spinning is quick, large scale, and free of high voltages and metallic targets. We believe that our new strategy toward producing transparent air filters will be useful for generating a real commercial device for achieving a healthier indoor environment.

Methods. Blowspinning. The solution systems of the polymers used in the present work include 10 wt % of PAN (MW = 1.5×10^5 g mol⁻¹; Aldrich) in dimethylformamide (DMF), 10 wt % of polyvinylpyrrolidone (MW = 1.3×10^6 g mol⁻¹; Alfa Aesar) in ethanol, 30 wt % of poly(methyl methacrylate) (PMMA) (MW = 3.3×10^4 g mol⁻¹; Aladdin) in dimethylformamide (DMF), and 30 wt % of Nylon-66 in formic acid. All of the polymeric solutions were loaded in a 1 ml syringe with a 22 gauge needle bend tip. The syringe was fitted in a syringe pump, and the bend tip was adjusted in front of a continuously air blowing hollow pipe. Blow-spun fibers were collected on the copper window screen with 0.008 mm wire thickness and 1 × 1 mm mesh size. The blow-spun nanofibers would lie across the screen mesh to form the air filter. The applied pressure, the pump rate, the blow-spinning duration, and the needle-to-collector distance were carefully adjusted to control the nanofiber diameter and packing density. A similar approach was adopted with slight amendments in experimental setup for both the window screen coating and for roll-to-roll manufacturing of nanofibers onto a rolling mesh with multi-needles.

Transparency Measurements. Optical transmittance for all samples was carried out on Shimadzu UV-vis spectrophotometer (UV-2600) with a halogen lamp as light source and R-928 photomultiplier detector. The samples were placed in front of integrated light-based spheres. For air filters coated with blow-spun fibers on copper mesh, a clean copper mesh of similar dimensions was placed as reference. The transmittance spectrum was recorded from 400 to 800 nm and the average transmittance was measured.

PM-Based Removal Efficiency Test. For all PM removal tests, sample PM particles were produced by burning incense smoke. This model experimental smoke contained a wide distribution of PM particles from <300 nm to >10 μm with most of the particles being <1 μm. The smoke concentration was adjusted by altering the specific amount of time incense was burned to achieve a PM_{2.5} index >300. The concentration and number of PM particles for all ranges of sizes were detected and calculated by CEM counter. The removal efficiencies were simply calculated by comparing the PM numbers before and after filtration.

Characterization. SEM images were taken with a Carl Zeiss microscope with accelerating voltages of 5 kV. XPS elemental analysis of smoke PM was carried out on a Thermo Fisher, ESCA Lab 250 spectrometer using a monochromatized Al Kα X-ray source. Fourier transform infrared spectroscopy (FTIR) was conducted by a Nicolet 6700 FTIR Thermo Specific spectrophotometer from 400 to 4000 cm⁻¹ under a vacuum.

■ ASSOCIATED CONTENT

● Supporting Information

The Supporting Information is available free of charge on the ACS Publications website at DOI: 10.1021/acs.nanolett.6b04771.

Fiber diameter changes, PM removal efficiencies, SEM images, and comparison of air filter characteristics (PDF) Video of sequential 4-needle blow spinning of uniform nanofibers continuously coating on a rolling nylon mesh (AVI)

■ AUTHOR INFORMATION

Corresponding Authors

*E-mail: huiwu@tsinghua.edu.cn

*E-mail: yicui@stanford.edu

ORCID

Xiaopeng Bai: 0000-0002-5769-9700

Hui Wu: 0000-0002-4284-5541

Author Contributions

§B.K. and X.B. contributed equally to this work.

Notes

The authors declare no competing financial interest.

■ ACKNOWLEDGMENTS

This study was supported by the National Basic Research of China (Grant Nos. 2015CB932500 and 2013CB632702) and the NSF of China (Grant No. 51302141).

■ REFERENCES

- (1) Zhang, R.; Jing, J.; Tao, J.; Hsu, S. C.; Wang, G.; Cao, J.; Lee, C. S. L.; Zhu, L.; Chen, Z.; Zhao, Y.; Shen, Z. *Atmos. Chem. Phys.* **2013**, *13*, 7053–7074.
- (2) Watson, J. G. *J. Air Waste Manage. Assoc.* **2002**, *52*, 628–71.
- (3) Streets, D. G.; Wu, Y.; Chin, M. *Geophys. Res. Lett.* **2006**, *33*, L15806.
- (4) Andreae, M. O.; Rosenfeld, D. *Earth-Sci. Rev.* **2008**, *89*, 13–41.
- (5) Mahowald, N. *Science* **2011**, *334*, 794–796.
- (6) Horton, D. E.; Skinner, C. B.; Singh, D.; Diffenbaugh, N. S. *Nat. Clim. Change* **2014**, *4*, 698–703.
- (7) Nel, A. *Science* **2005**, *308*, 804–806.
- (8) Harrison, R. M.; Yin, J. X. *Sci. Total Environ.* **2000**, *249*, 85–101.
- (9) Pope, C. A.; Dockery, D. W. *J. Air Waste Manage. Assoc.* **2006**, *56*, 709–742.
- (10) Betha, R.; Behera, S. N.; Balasubramanian, R. *Environ. Sci. Technol.* **2014**, *48*, 4327–4335.
- (11) Wu, S. W.; Deng, F. R.; Wei, H. Y.; Huang, J.; Wang, X.; Hao, Y.; Zheng, C. J.; Qin, Y.; Lv, H. B.; Shima, M.; Guo, X. B. *Environ. Sci. Technol.* **2014**, *48*, 3438–3444.
- (12) Brook, R. D.; Rajagopalan, S.; Pope, C. A.; Brook, J. R.; Bhatnagar, A.; Diez-Roux, A. V.; Holguin, F.; Hong, Y. L.; Luepker, R. V.; Mittleman, M. A.; Peters, A.; Siscovick, D.; Smith, S. C.; Whitsel, L.; Kaufman, J. D.; Epidemiol, A. H. A. C.; Dis, C. K. C.; Metab, C. N. P. A. *Circulation* **2010**, *121*, 2331–2378.
- (13) Anenberg, S. C.; Horowitz, L. W.; Tong, D. Q.; West, J. J. *Environ. Health Perspect.* **2010**, *118*, 1189–1195.
- (14) Timonen, K. L.; Vanninen, E.; De Hartog, J.; Ibaldo-Mulli, A.; Brunekreef, B.; Gold, D. R.; Heinrich, J.; Hoek, G.; Lanki, T.; Peters, A.; Tarkiainen, T.; Tiittanen, P.; Kreyling, W.; Pekkanen, J. J. *J. Exposure Sci. Environ. Epidemiol.* **2006**, *16*, 332–341.
- (15) Hinds, W. C. *Aerosol Technology: Properties, Behavior, and Measurement of Airborne Particles*; Wiley-Interscience: New York, 1982; Vol. 1.
- (16) US Department of Energy's Office of Energy Efficiency and Renewable Energy *2010 Buildings Energy Data Book*; D&R International Ltd., 2011).
- (17) Bruce, N.; Perez-Padilla, R.; Albalak, R. *World Health Organ.* **2000**, *78*, 1078–1092.
- (18) Wang, H.; Zhuang, Y.; Wang, Y.; Sun, Y.; Yuan, H.; Zhuang, G.; Hao, Z. *J. Environ. Sci.* **2008**, *20*, 1323–1327.
- (19) Platt, S. M.; Haddad, I. E.; Pieber, S. M.; Huang, R. J.; Zardini, A. A.; Clairotte, M.; Suarez-Bertoa, R.; Barmet, P.; Pfaffenberger, L.; Wolf, R.; et al. *Nat. Commun.* **2014**, *5*, 3749.
- (20) Han, X. L.; Naeher, L. P. *Environ. Int.* **2006**, *32*, 106–120.
- (21) Maricq, M. M. *J. Aerosol Sci.* **2007**, *38*, 1079–1118.
- (22) Liu, C.; Hsu, P. C.; Lee, H. W.; Ye, M.; Zheng, G.; Liu, N.; Li, W.; Cui, Y. *Nat. Commun.* **2015**, *6*, 6205.

- (23) Xu, J.; Liu, C.; Hsu, P. C.; Liu, K.; Zhang, R.; Liu, Y.; Cui, Y. *Nano Lett.* **2016**, *16*, 1270–1275.
- (24) Zhang, R.; Liu, C.; Hsu, P. C.; Zhang, C.; Liu, N.; Zhang, J.; Lee, R. J.; Lu, Y.; Qiu, Y.; Chu, S.; Cui, Y. *Nano Lett.* **2016**, *16*, 3642–3649.
- (25) Mcintrye, J. E.; Nakajima, T. *Advanced Fiber Spinning Technology*; Technomic Publishing Co.: Lancaster, 1994.
- (26) Kayser, J.; Shambaugh, R. L. *Polym. Eng. Sci.* **1990**, *30*, 1237–1251.
- (27) Lin, T. C.; Krishnaswamy, G.; Chi, D. S. *Clin. Mol. Allergy* **2008**, *6*, 3–3.
- (28) Huang, R. J.; Zhang, Y.; Bozzetti, C.; Ho, K. F.; Cao, J. J.; Han, Y.; Daellenbach, K. R.; Slowik, J. G.; Platt, S. M.; Canonaco, F.; et al. *Nature* **2014**, *514*, 218–222.